ICFP M2 Advanced Quantum Mechanics
Homework: Ultracold Fermi gas in the BCS regime
Solutions to selected questions

D.J. Papoular

December 19, 2024

1 Question 2: The role of the centrifugal barrier

The system we consider is a gas of fermionic alkali atoms (e.g. ^{6}Li or ^{40}K), in the presence of a weakly attractive interaction between atoms of opposite spins. In the absence of interaction, the many–body ground state of this system is a Fermi sea, characterised by the Fermi energy E_F (i.e. the energy of the highest–occupied single–particle state) and the corresponding Fermi wavevector k_F, defined by $E_F = \hbar^2 k_F^2/(2m)$ with m being the mass of a single atom. We focus on the case of very low temperatures, and we assume that the Fermi sea is not altogether destroyed by the weak attraction: this will be confirmed by subsequent calculations described e.g. in Section 5 below. Then, interaction effects dominantly involves atoms whose energies lie in a narrow range comprising E_F. Typically, the Fermi temperature $T_F = E_F/k_\mathrm{B}$ is of the order of 1μK, and the temperature of the gas is $T \approx 0.05\,T_F = 50\,$nK [1, §2.1, Table II].

We focus on two atoms near the Fermi surface, undergoing a low–energy collision with an energy of the order of E_F. The Schrödinger for the relative motion of the two colliding atoms reads:

$$-\frac{\hbar^2}{2m_\mathrm{red}}\,\Delta\phi \quad + \quad V_\mathrm{int}(r)\,\phi \quad = \quad E\,\phi\;. \tag{1}$$

In Eq. (1), the wavefunction $\phi(\boldsymbol{r})$ depends on the relative coordinate $\boldsymbol{r} = \boldsymbol{r}_1 - \boldsymbol{r}_2$, the Laplacian Δ is taken with respect to $\boldsymbol{r}$, the reduced mass $m_\mathrm{red} = m^2/(2m) = m/2$, and the energy E characterises the relative motion. We now consider, in turn, the interaction term $V_\mathrm{int}(\boldsymbol{r})\,\phi(\boldsymbol{r})$, and the kinetic energy term proportional to $\Delta\phi$.

Interaction term. The interaction potential $V_\mathrm{int}(r)$ arises from the energy of the electron terms. The atomic nuclei are much heavier than the outer electrons (mass ratio $\sim 10^4$ for ^{6}Li atoms), therefore the electron terms are calculated in the Born–Oppenheimer approximation, whereby the nuclei are assumed to be fixed at a given distance r. For neutral atoms, V_int depends on $r = |\boldsymbol{r}|$ only. For smaller distances, $V_\mathrm{int}(r)$ depends on the total two–atom spin $S = 0$ (singlet potential) or S=1 (triplet potential) due to exchange effects [2, chap. 32]. However, these decrease exponentially with increasing distance, and they are negligible for the distances at play in the centrifugal effect considered here, so that V_int is simply a function of r with no spin dependence. It is well represented by the attractive van der Waals 'tail'

$$V_\mathrm{int}(r) \quad = \quad -C_6/r^6\;, \qquad \text{where the interaction strength } C_6 > 0. \tag{2}$$

For instance, for ^{6}Li [3, Table I], $C_6 = 1390\,E_\mathrm{H} a_0^6$, where[1] E_H is the Hartree energy and a_0 is the Bohr radius.

Kinetic energy term. The direction of the incident atoms sets a specific direction in space about with the collisional problem exhibits cylindrical symmetry. However, thanks to the spherical symmetry of $V_\mathrm{int}(r)$, the scattering state $\phi(\boldsymbol{r})$ may be expanded into a series of partial waves [4, Sec. VIII-C-3] of the form $R_l(r)\,Y_l^m(\theta,\phi)$, with Y_l^m being the spherical harmonic corresponding to the integer quantum numbers l and m. Each of the terms in this sum is a simultaneous eigenstate of three operators: *(i)* the Hamiltonian H describing the relative motion (eigenvalue: the energy E); *(ii)* the squared modulus $\boldsymbol{\ell}^2 = l_x^2 + l_y^2 + l_z^2$ of the angular momentum operator (eigenvalue: $l(l+1)\,\hbar^2$), and *(iii)* the operator l_z representing the angular momentum along the quantisation axis z (eigenvalue: $m\,\hbar$). We focus on one such term $R_l(r)$, and use the following representation of the Laplacian in spherical cooordinates:

$$\Delta f(\boldsymbol{r}) \quad = \quad \frac{1}{r}\frac{\partial^2}{\partial r^2}(rf) \quad - \quad \frac{\boldsymbol{\ell}^2}{r^2}\,f\;, \quad \text{valid for } r > 0. \tag{3}$$

---

[1] The Hartree energy $E_\mathrm{H} = 4.36 \times 10^{-18}$ J, the Bohr radius $a_0 = 5.29 \times 10^{-11}$ m, and the electron mass $m_e = 9.11 \times 10^{-31}$ kg make up the atomic unit system, often used to describe low–energy atomic scattering phenomena. They are related through $E_\mathrm{H} = \hbar^2/(m_e a_0^2)$.

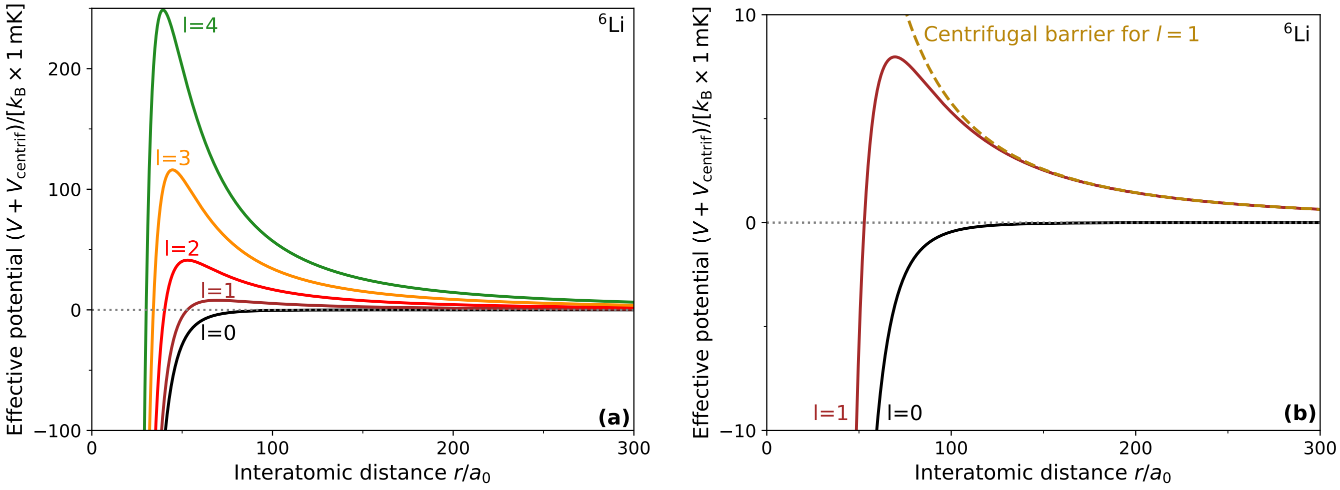

Figure 1 Total effective potential $V_{\text{int}}(r) + V_{\text{centrif}}(r)$, appearing in the Schrödinger equation governing the behaviour of the radial wave function u_l, represented for ^{6}Li atoms. **(a)** The effective potential exhibits a maximum for each $l > 0$, leading to the centrifugal barrier. **(b)** Zoom–in onto the partial waves with $l = 0$ (black curve, no barrier) and $l = 1$ (brown curve, the barrier is present). The dashed golden curve shows $V_{\text{centrif}}(r)$ for $l = 1$.

Introducing the function $u_l(r)$ such that $R_l(r) = u_l(r)/r$, and combining Eqs. (1) and (3), we obtain:

$$-\frac{\hbar^2}{2m_{\text{red}}}\frac{\partial^2 u_l}{\partial r^2} \quad + \quad \left[\frac{\hbar^2\, l(l+1)}{2m_{\text{red}}\, r^2} \quad + \quad V_{\text{int}}(r)\right] u_l \quad = \quad E\, u_l \ . \tag{4}$$

Equation (4) shows that the function $u_l(r)$ satisfies a one–dimensional Schrödinger equation involving the effective potential $[V_{\text{int}}(r) + V_{\text{centrif}}]$, where the term $V_{\text{centrif}} = \hbar^2\, l(l+1)/(2m_{\text{red}} r^2)$. If the quantum number $l = 0$ ('s–wave' component: 's' like 'sharp' and like 'spherical'), the term V_{centrif} vanishes. However, for all higher partial waves, characterised by the integer quantum numbers $l > 0$, $V_{\text{centrif}}(r)$ is the *centrifugal barrier*, which is repulsive.

Total effective potential. The total effective potential is shown on Fig. 1(a), in the case of ^{6}Li, for the lowest partial waves $l = 0$ to 4. For each value of l, it exhibits a maximum, whose position $r_{\max}$ and value $V_{\max}$ may be calculated using the van der Waals approximation to $V_{\text{int}}(r)$ given by Eq. (2):

$$r_{\max} \quad = \quad \left(\frac{3}{l(l+1)}\right)^{1/4} l_{\text{vdw}} \qquad \text{and} \qquad V_{\max} \quad = \quad 2\left(\frac{l(l+1)}{3}\right)^{3/2} E_{\text{vdw}} \ . \tag{5}$$

In Eq. (5), $l_{\text{vdw}} = (mC_6/\hbar^2)^{1/4}$ and $E_{\text{vdw}} = [\hbar^6/(m^3 C_6)]^{1/2}$ are the van der Waals length and energy[2]. For ^{6}Li atoms, the barrier height for $l = 1$ is of the order of 8 mK (maximum of the brown curve on Fig. 1(b)). Furthermore, for all incident energies $E \lesssim 2\,m$K, the interaction $V_{\text{int}}(r)$ is negligible compared to the centrifugal term $V_{\text{centrif}}(r)$. Hence, for such incident energies, the interaction plays no role[3] for partial waves $l \leq 1$, and the centrifugal barrier prevents the atoms from coming close enough to be affected by it.

***s*–wave superfluidity.** The temperature ($T = 50\,$nK) and Fermi temperature ($T_F = 1\,\mu$K) in typical experiments on weakly attractive Fermi gases are much smaller than the barrier height for $l = 1$. Therefore, interaction plays no role in all partial waves other than the s–wave. The paring mechanism which underlies superfluidity hinges on the presence of interaction, so that its dominant contribution comes from the s–wave component. In this case, $l = 0$, so that the relevant spherical harmonic $Y_0^0 = 1/\sqrt{4\pi}$ is a constant. Hence, the corresponding wavefunction for the relative motion is spherically symmetric. Consequently, the *spatial* wavefunction for the two particles is symmetric under the exchange of the two particles. For fermions, the *full (i.e. spatial and spin)* wavefunction must be antisymmetric under the exchange of the particles. Hence, the two–particle *spin state* must be chosen to be antisymmetric, i.e. it must be the singlet state $|\chi_{12}\rangle = (|{\uparrow\downarrow}\rangle - |{\downarrow\uparrow}\rangle)/\sqrt{2}$.

---

[2] Beware: some authors include dimensionless numerical prefactors in their definitions of l_{vdw} and E_{vdw}: see e.g. Ref. [3, Eq. 13].

[3] This simple conclusion is invalid in the presence of a 'shape' resonance [5, Sec. II.B.1].

2 Question 3: Second–quantised expression for $|\Psi_N\rangle$

We consider the wavefunction $|\Psi_N\rangle$, representing a well–defined number N of atoms, paired into $N/2$ Cooper pairs:

$$\Psi_N(\boldsymbol{r}_1,\ldots,\boldsymbol{r}_N) = \mathcal{A}\left[\phi(\boldsymbol{r}_1,\boldsymbol{r}_2)\,|\chi_{12}\rangle\,,\ldots\phi(\boldsymbol{r}_{N-1},\boldsymbol{r}_N)\,|\chi_{N-1,N}\rangle\right]\ , \tag{6}$$

where the antisymmetriser $\mathcal{A}$ acts on all fermionic coordinates, and $\phi(\boldsymbol{r}_i,\boldsymbol{r}_j)$ is the spatial wavefunction of the pair involving the fermions i and j. We choose the two–fermion internal state $|\chi_{ij}\rangle = (|{\uparrow\downarrow}\rangle - |{\downarrow\uparrow}\rangle)/\sqrt{2}$ to be the singlet state so that it is antisymmetric, which ensures that the spatial wavefunction $\phi(\boldsymbol{r}_i,\boldsymbol{r}_j)$ is symmetric and, hence, allows for s–wave pairing. The wavefunction $|\Psi_N\rangle$ is antisymmetric and normalised to unity:

$$\langle\Psi_N|\Psi_N\rangle = \int d^3r_1\ldots d^3r_N\,|\Psi_N(\boldsymbol{r}_1,\ldots,\boldsymbol{r}_N)|^2 = 1\ . \tag{7}$$

In order to write $|\Psi_N\rangle$ in second–quantised form, we introduce the pair creation operator $b^\dagger$:

$$b^\dagger = \int d^3r_1 d^3r_2\,\phi(\boldsymbol{r}_1,\boldsymbol{r}_2)\,\hat{\Psi}^\dagger_\uparrow(\boldsymbol{r}_1)\hat{\Psi}^\dagger_\downarrow(\boldsymbol{r}_2)\ , \tag{8}$$

where the field operator $\hat{\Psi}_\sigma(\boldsymbol{r})$ creates a particle with the spin $\sigma =\uparrow$ or $\downarrow$ at the point $\boldsymbol{r}$.

2.1 A single Cooper pair

We first consider the action of $b^\dagger$ on the vacuum state $|\text{vac}\rangle$:

$$b^\dagger\,|\text{vac}\rangle = \int d^3r_1 d^3r_2\,\phi(\boldsymbol{r}_1,\boldsymbol{r}_2)\,\hat{\Psi}^\dagger_\uparrow(\boldsymbol{r}_1)\hat{\Psi}^\dagger_\downarrow(\boldsymbol{r}_2)\,|\text{vac}\rangle \quad = \int d^3r_1 d^3r_2\,\phi(\boldsymbol{r}_1,\boldsymbol{r}_2)\,|\boldsymbol{r}_1\uparrow,\boldsymbol{r}_2\downarrow\rangle\ . \tag{9}$$

The ket $|\boldsymbol{r}_1\uparrow,\boldsymbol{r}_2\downarrow\rangle$ appearing in the right–hand side of Eq. (9) is written in second–quantised notation. It is a two–fermion state which is properly antisymmetrised, and whose first–quantised expression is:

$$|\boldsymbol{r}_1\uparrow,\boldsymbol{r}_2\downarrow\rangle = \frac{1}{\sqrt{2}}\left(|1:\boldsymbol{r}_1\uparrow,2:\boldsymbol{r}_2\downarrow\rangle - |1:\boldsymbol{r}_2\downarrow,2:\boldsymbol{r}_1\uparrow\rangle\right)\ . \tag{10}$$

Replacing Eq. (10) into Eq. (9), we obtain:

$$b^\dagger\,|\text{vac}\rangle = \int d^3r_1 d^3r_2\,\phi(\boldsymbol{r}_1,\boldsymbol{r}_2)\,\frac{1}{\sqrt{2}}\left(|1:\boldsymbol{r}_1\uparrow,2:\boldsymbol{r}_2\downarrow\rangle - |1:\boldsymbol{r}_2\downarrow,2:\boldsymbol{r}_1\uparrow\rangle\right)\ . \tag{11}$$

We exchange the role of the integration variables $\boldsymbol{r}_1$ and $\boldsymbol{r}_2$ in the term involving $|1:\boldsymbol{r}_2\downarrow,2:\boldsymbol{r}_1\uparrow\rangle$ Recalling that $\phi(\boldsymbol{r}_1,\boldsymbol{r}_2)=\phi(\boldsymbol{r}_2,\boldsymbol{r}_1)$, we obtain:

$$\begin{aligned} b^\dagger\,|\text{vac}\rangle &= \int d^3r_1 d^3r_2\,\phi(\boldsymbol{r}_1,\boldsymbol{r}_2)\,\frac{1}{\sqrt{2}}\left(|1:\boldsymbol{r}_1\uparrow,2:\boldsymbol{r}_2\downarrow\rangle - |1:\boldsymbol{r}_1\downarrow,2:\boldsymbol{r}_2\uparrow\rangle\right) &(12)\\ &= \left[\int d^3r_1 d^3r_2\,\phi(\boldsymbol{r}_1,\boldsymbol{r}_2)\,|1:\boldsymbol{r}_1,2:\boldsymbol{r}_2\rangle\right]|\chi_{12}\rangle\ , &(13)\end{aligned}$$

where we have factorised the spatial and internal–state parts of the wavefunction. Hence, $b^\dagger\,|\text{vac}\rangle$ is the properly normalised and antisymmetric wavefunction for a single Cooper pair.

2.2 $N/2$ Cooper pairs

We now wish to write the wavefunction $|\Psi_N\rangle$ in terms of $b^\dagger$. This wavefunction consists of N atoms and, hence, of $N/2$ Cooper pairs. Therefore, we consider:

$$b^{\dagger N/2}\,|\text{vac}\rangle = \int d^3r_1\ldots d^3r_N\,\phi(\boldsymbol{r}_1,\boldsymbol{r}_2)\ldots\phi(\boldsymbol{r}_{N-1},\boldsymbol{r}_N)\,|\boldsymbol{r}_1\uparrow,\boldsymbol{r}_2\downarrow,\ldots,\boldsymbol{r}_{N-1}\uparrow,\boldsymbol{r}_N\downarrow\rangle\ , \tag{14}$$

where the ket $|\boldsymbol{r}_1\uparrow,\boldsymbol{r}_2\downarrow,\ldots,\boldsymbol{r}_{N-1}\uparrow,\boldsymbol{r}_N\downarrow\rangle$ is written in second–quantised notation, so that the indices on the variables $\boldsymbol{r}_1$, …, $\boldsymbol{r}_N$ have nothing to do with particle ordering. The wavefunction $b^{\dagger N/2}\,|\text{vac}\rangle$ is a superposition of antisymmetrised wavefunctions, hence, it is itself antisymmetrised. Therefore, it is equal to $|\Psi_N\rangle$ up to a normalisation factor.

We now calculate the norm of $b^{\dagger N/2}\,|\mathrm{vac}\rangle$:

$$\begin{aligned}\langle\mathrm{vac}|b^{N/2}b^{\dagger N/2}|\mathrm{vac}\rangle = &\int d^3r_1\ldots d^3r_N \int d^3r'_1\ldots d^3r'_N \\ &\phi^*(\boldsymbol{r}'_1,\boldsymbol{r}'_2)\ldots\phi^*(\boldsymbol{r}'_{N-1},\boldsymbol{r}'_N)\,\phi(\boldsymbol{r}_1,\boldsymbol{r}_2)\ldots\phi(\boldsymbol{r}_{N-1},\boldsymbol{r}_N) \\ &\langle \boldsymbol{r}'_1\uparrow,\boldsymbol{r}'_2\downarrow,\ldots,\boldsymbol{r}'_{N-1}\uparrow,\boldsymbol{r}'_N\downarrow \;|\; \boldsymbol{r}_1\uparrow,\boldsymbol{r}_2\downarrow,\ldots,\boldsymbol{r}_{N-1}\uparrow,\boldsymbol{r}_N\downarrow\rangle\ . \end{aligned} \tag{15}$$

If the pairs appearing in the bra $\langle(\boldsymbol{r}'_1,\boldsymbol{r}'_2),\ldots,(\boldsymbol{r}'_{N-1},\boldsymbol{r}'_N)|$ match those appearing in the ket $|(\boldsymbol{r}_1,\boldsymbol{r}_2),\ldots,(\boldsymbol{r}_{N-1},\boldsymbol{r}_N)\rangle$ up to a permutation of the $N/2$ pairs the scalar product between the two N–particle states on the last line of Eq. (15) is non–zero. There are $(N/2)!$ such transpositions. For each of them, the scalar product is equal to the product of N Dirac peaks $\delta(\boldsymbol{r}_1-\boldsymbol{r}'_1)\cdots\delta(\boldsymbol{r}_N-\boldsymbol{r}'_N)$. The expression for $|\Psi_N\rangle$ put forward in question 3 of the problem set is obtained by neglecting[4] the contributions of the permutations which mix the pairs $(\boldsymbol{r}_{2i-1},\boldsymbol{r}_{2i})$ among each other. Then, Eq. (15) reduces to:

$$\langle\mathrm{vac}|b^{N/2}b^{\dagger N/2}|\mathrm{vac}\rangle = (N/2)!\int d^3r_1 d^3r_2\,|\phi(\boldsymbol{r}_1,\boldsymbol{r}_2)|^2\cdots\int d^3r_{N-1}d^3r_N\,|\phi(\boldsymbol{r}_{N-1},\boldsymbol{r}_N)|^2 \quad = (N/2)! \tag{16}$$

Thus, the norm of $b^{\dagger N/2}\,|\mathrm{vac}\rangle$ is $\sqrt{(N/2)!}$, and $|\Psi_N\rangle$ is expressed in terms of $b^\dagger$ as follows:

$$|\Psi_N\rangle = \frac{b^{\dagger N/2}}{\sqrt{(N/2)!}}\,|\mathrm{vac}\rangle\ , \tag{17}$$

where the numerical prefactor is the same as for a true bosonic creation operator.

3 Questions 7–9: The BCS wavefunction

3.1 The many–particle Hilbert space

We consider the BCS wavefunction $|\Psi_{\mathrm{BCS}}\rangle$, defined by Eq. 6 in the problem set:

$$|\Psi_{\mathrm{BCS}}\rangle = \frac{1}{\mathcal{N}}\exp\left(\sqrt{N_p}\,b^\dagger\right)|\mathrm{vac}\rangle\ , \tag{18}$$

where $N_p = N/2$ is the average number of pairs, which is one half of the average number of particles $N = \langle\hat{N}\rangle$, $b^\dagger = \sum_{\boldsymbol{k}}\phi_k\,c^\dagger_{\boldsymbol{k}\uparrow}c^\dagger_{-\boldsymbol{k}\downarrow}$ is the creation operator for a Cooper pair, and the (real and positive) number $\mathcal{N}$ is a normalisation factor which ensures that $\langle\Psi_{\mathrm{BCS}}|\Psi_{\mathrm{BCS}}\rangle = 1$. The state $|\Psi_{\mathrm{BCS}}\rangle$ does not have a well–defined particle number, hence, the Hilbert space $\mathcal{H}$ it belongs to is best described in the language of second quantisation.

The Hilbert space $\mathcal{H}$ is usually decomposed into subspaces $\mathcal{H}_n$ with well–defined particle numbers n:

$$\mathcal{H} = \mathcal{H}_0\oplus\mathcal{H}_1\oplus\mathcal{H}_2\oplus\cdots \quad = \bigoplus_n \mathcal{H}_n\ . \tag{19}$$

In Eq. (19), $\mathcal{H}$ is written in terms of the subspaces $\mathcal{H}_n$ as a direct sum, because if $|\psi_{n_1}\rangle$ is a valid n_1–particle quantum state (i.e. an element of $\mathcal{H}_{n_1}$) and $|\psi_{n_2}\rangle$ is a valid n_2–particle quantum state (i.e. an element of $\mathcal{H}_{n_2}$), then both $|\psi_{n_1}\rangle$ and $|\psi_{n_2}\rangle$ are valid elements of $\mathcal{H}$, and the superposition state $(|\psi_{n_1}\rangle+|\psi_{n_2}\rangle)/\sqrt{2}$ is also a valid quantum state.

In the context of BCS theory, the decomposition of $\mathcal{H}$ in terms of particle numbers is not the most adequate one: it is more convenient to decompose $\mathcal{H}$ in terms of spatial modes. We first consider the plane–wave state $|\boldsymbol{k}\rangle$. Because of Pauli's exclusion principle, there are only four licit fermionic states that may be constructed from this spatial state, which may be non–populated ($|\mathrm{vac}_{\boldsymbol{k}}\rangle$), or populated by a single particle ($|\boldsymbol{k}\uparrow\rangle$ or $|\boldsymbol{k}\downarrow\rangle$), or populated by two particles ($|\boldsymbol{k}\uparrow,\boldsymbol{k}\downarrow\rangle$). We call $\mathcal{H}^0_{\boldsymbol{k}}$ the four–dimensional Hilbert space spanned by these four states. Then, the complete many–body Hilbert space $\mathcal{H}$ is the tensor product of the spaces $\mathcal{H}^0_k$ over all plane–wave indices $\boldsymbol{k}$:

$$\mathcal{H} = \bigotimes_{\boldsymbol{k}}\mathcal{H}^0_{\boldsymbol{k}}\ . \tag{20}$$

This new decomposition of $\mathcal{H}$ *involves tensor products and not direct sums*, because it involves independent spatial modes which may be independently populated. For instance, let us consider two different plane–wave states $|\boldsymbol{k}_1\rangle$ and $|\boldsymbol{k}_2\rangle$. Then, $|\boldsymbol{k}_1\uparrow\rangle$ is a single–mode state, which is an element of $\mathcal{H}^0_{\boldsymbol{k}_1}$, and $|\boldsymbol{k}_2\uparrow,\boldsymbol{k}_2\downarrow\rangle$ is another single–mode state, which is an element of $\mathcal{H}^0_{\boldsymbol{k}_2}$; these two states may be combined to obtain an element of $\mathcal{H}$ which is $|\boldsymbol{k}_1\uparrow\rangle\otimes|\boldsymbol{k}_2\uparrow,\boldsymbol{k}_2\downarrow\rangle = |\boldsymbol{k}_1\uparrow,\boldsymbol{k}_2\uparrow,\boldsymbol{k}_2\downarrow\rangle$, and which contains two populated modes[5].

---

[4] The exact normalisation of the state $|\Psi_N\rangle$ is a difficult problem: see e.g. [1, §4.4] and references therein.

[5] One may also consider the superposition $(|\boldsymbol{k}_1\uparrow\rangle+|\boldsymbol{k}_2\uparrow,\boldsymbol{k}_2\downarrow\rangle)/\sqrt{2} = (|\boldsymbol{k}_1\uparrow\rangle\otimes|\mathrm{vac}_{\boldsymbol{k}_2}\rangle+|\mathrm{vac}_{\boldsymbol{k}_1}\rangle\otimes|\boldsymbol{k}_2\uparrow,\boldsymbol{k}_2\downarrow\rangle)/\sqrt{2}$.

The most convenient decomposition of $\mathcal{H}$ in the context of BCS theory is a variant of Eq. (20). We wish the elementary Hilbert spaces $\mathcal{H}_{\boldsymbol{k}}$ to encode the presence or the absence of Cooper pairs, each of which consists of one atom in the state $|\boldsymbol{k}\uparrow\rangle$ and another in the state $|-\boldsymbol{k}\downarrow\rangle$. Hence, instead of using the spaces $\mathcal{H}^0_{\boldsymbol{k}}$, we introduce the four–dimensional spaces $\mathcal{H}_{\boldsymbol{k}}$ spanned by the states $|\mathrm{vac}_{\boldsymbol{k}\uparrow,-\boldsymbol{k}\downarrow}\rangle$, $|\boldsymbol{k}\uparrow\rangle$, $|-\boldsymbol{k}\downarrow\rangle$, and $|\boldsymbol{k}\uparrow,-\boldsymbol{k}\downarrow\rangle$. Here, the vacuum state $|\mathrm{vac}_{\boldsymbol{k}\uparrow,-\boldsymbol{k}\downarrow}\rangle$ should be understood as the absence of any particle in the states $|\boldsymbol{k}\uparrow\rangle$ and $|-\boldsymbol{k}\downarrow\rangle$. We may finally write:

$$\mathcal{H} = \bigotimes_{\boldsymbol{k}} \mathcal{H}_{\boldsymbol{k}} \ . \tag{21}$$

3.2 Factorisation of the BCS wavefunction

The commutator $[c^\dagger_{\boldsymbol{k}_1\uparrow}c^\dagger_{-\boldsymbol{k}_1\downarrow}, c^\dagger_{\boldsymbol{k}_2\uparrow}c^\dagger_{-\boldsymbol{k}_2\downarrow}] = 0$ for any two plane waves $|\boldsymbol{k}_1\rangle$ and $|\boldsymbol{k}_2\rangle$. Therefore, the exponential of the sum of operators in Eq. (18) may be written as a product of exponentials:

$$\mathcal{N}\,|\Psi_{\mathrm{BCS}}\rangle = \prod_{\boldsymbol{k}} \exp\left(\sqrt{N_p}\,\phi_k\, c^\dagger_{\boldsymbol{k}\uparrow}c^\dagger_{-\boldsymbol{k}\downarrow}\right)|\mathrm{vac}\rangle \ . \tag{22}$$

Now, we recall that $c^\dagger_{\boldsymbol{k}\uparrow}$ and $c^\dagger_{-\boldsymbol{k}\downarrow}$ are fermionic operators, so that $c^{\dagger 2}_{\boldsymbol{k}\uparrow} = 0$ and $c^{\dagger 2}_{-\boldsymbol{k}\downarrow} = 0$. The exponential appearing in Eq. (22) is a series involving the integer powers $(c^\dagger_{\boldsymbol{k}\uparrow}c^\dagger_{-\boldsymbol{k}\downarrow})^n$, which are all zero for $n \geq 2$. Therefore, one may replace each exponential in Eq. (22) by the only two surviving terms, which leads to:

$$\mathcal{N}\,|\Psi_{\mathrm{BCS}}\rangle = \prod_{\boldsymbol{k}} \left(1 + \sqrt{N_p}\,\phi_k\, c^\dagger_{\boldsymbol{k}\uparrow}c^\dagger_{-\boldsymbol{k}\downarrow}\right)|\mathrm{vac}\rangle \ . \tag{23}$$

Now, we shall factorise $|\Psi_{\mathrm{BCS}}\rangle$ into a form which is compatible with the decomposition of Eq. (21). The vacuum state $|\mathrm{vac}\rangle$ appearing in Eq. (23) is the product of all vacuum states $|\mathrm{vac}_{\boldsymbol{k}\uparrow,-\boldsymbol{k}\downarrow}\rangle$:

$$|\mathrm{vac}\rangle = \prod_{\boldsymbol{k}} |\mathrm{vac}_{\boldsymbol{k}\uparrow,-\boldsymbol{k}\downarrow}\rangle \ . \tag{24}$$

Furthermore, for two different wavevectors $\boldsymbol{k}_1$ and $\boldsymbol{k}_2$ and any two complex numbers $\alpha_{\boldsymbol{k}_1}$ and $\alpha_{\boldsymbol{k}_2}$,

$$\begin{aligned}
&\left(1 + \alpha_{\boldsymbol{k}_1} c^\dagger_{\boldsymbol{k}_1\uparrow}c^\dagger_{-\boldsymbol{k}_1\downarrow}\right)\left(1 + \alpha_{\boldsymbol{k}_2} c^\dagger_{\boldsymbol{k}_2\uparrow}c^\dagger_{-\boldsymbol{k}_2\downarrow}\right)|\mathrm{vac}_{\boldsymbol{k}_1\uparrow,-\boldsymbol{k}_1\downarrow}\rangle\,|\mathrm{vac}_{\boldsymbol{k}_2\uparrow,-\boldsymbol{k}_2\downarrow}\rangle && (25)\\
&= \left(1 + \alpha_{\boldsymbol{k}_1} c^\dagger_{\boldsymbol{k}_1\uparrow}c^\dagger_{-\boldsymbol{k}_1\downarrow}\right)\left(|\mathrm{vac}_{\boldsymbol{k}_1\uparrow,-\boldsymbol{k}_1\downarrow}\rangle\,|\mathrm{vac}_{\boldsymbol{k}_2\uparrow,-\boldsymbol{k}_2\downarrow}\rangle + \alpha_{\boldsymbol{k}_2}\,|\mathrm{vac}_{\boldsymbol{k}_1\uparrow,-\boldsymbol{k}_1\downarrow}\rangle\, c^\dagger_{\boldsymbol{k}_2\uparrow}c^\dagger_{-\boldsymbol{k}_2\downarrow}\,|\mathrm{vac}_{\boldsymbol{k}_2\uparrow,-\boldsymbol{k}_2\downarrow}\rangle\right) && (26)\\
&= \left[\left(1 + \alpha_{\boldsymbol{k}_1} c^\dagger_{\boldsymbol{k}_1\uparrow}c^\dagger_{-\boldsymbol{k}_1\downarrow}\right)|\mathrm{vac}_{\boldsymbol{k}_1\uparrow,-\boldsymbol{k}_1\downarrow}\rangle\right]\left[\left(1 + \alpha_{\boldsymbol{k}_2} c^\dagger_{\boldsymbol{k}_2\uparrow}c^\dagger_{-\boldsymbol{k}_2\downarrow}\right)|\mathrm{vac}_{\boldsymbol{k}_2\uparrow,-\boldsymbol{k}_2\downarrow}\rangle\right] \ . && (27)
\end{aligned}$$

Therefore, Eq. (23) may be rewritten as:

$$\mathcal{N}\,|\Psi_{\mathrm{BCS}}\rangle = \prod_{\boldsymbol{k}} \left[\left(1 + \sqrt{N_p}\,\phi_k\, c^\dagger_{\boldsymbol{k}\uparrow}c^\dagger_{-\boldsymbol{k}\downarrow}\right)|\mathrm{vac}_{\boldsymbol{k}\uparrow,-\boldsymbol{k}\downarrow}\rangle\right] \ . \tag{28}$$

Equation (28) is of the form $|\Psi_{\mathrm{BCS}}\rangle = \prod_{\boldsymbol{k}}|\Psi_{\boldsymbol{k}}\rangle$, where each $|\Psi_{\boldsymbol{k}}\rangle$ is an element of $\mathcal{H}_{\boldsymbol{k}}$ given by:

$$|\Psi_{\boldsymbol{k}}\rangle = \frac{1}{\mathcal{N}_{\boldsymbol{k}}}\left(|\mathrm{vac}_{\boldsymbol{k}\uparrow,-\boldsymbol{k}\downarrow}\rangle + \sqrt{N_p}\,\phi_k\;|\boldsymbol{k}\uparrow,-\boldsymbol{k}\downarrow\rangle\right) \ , \quad \text{with} \quad \mathcal{N} = \prod_{\boldsymbol{k}}\mathcal{N}_{\boldsymbol{k}} \ . \tag{29}$$

In order to normalise $|\Psi_{\mathrm{BCS}}\rangle$, it is sufficient to impose $\langle\Psi_{\boldsymbol{k}}|\Psi_{\boldsymbol{k}}\rangle = 1$ for all $\boldsymbol{k}$. This leads to $\mathcal{N}_k = \sqrt{1 + N_p|\phi_k|^2}$, so that we may finally write:

$$|\Psi_{\mathrm{BCS}}\rangle = \prod_{\boldsymbol{k}}\left(u_k\,|\mathrm{vac}_{\boldsymbol{k}\uparrow,-\boldsymbol{k}\downarrow}\rangle + v_k\,|\boldsymbol{k}\uparrow,-\boldsymbol{k}\downarrow\rangle\right) \ , \tag{30}$$

where u_k and v_k read:

$$u_k = \frac{1}{\sqrt{1 + N_p|\phi_k|^2}} \quad \text{and} \quad v_k = \frac{\sqrt{N_p}\,\phi_k}{\sqrt{1 + N_p|\phi_k|^2}} \ . \tag{31}$$

3.3 Interpretation of the BCS wavefunction

The factorisation $|\Psi_{\mathrm{BCS}}\rangle = \prod_{\boldsymbol{k}}|\Psi_{\boldsymbol{k}}\rangle$ provided by Eq. (30) allows for a simple physical interpretation of the BCS wavefunction, which may be understood as follows. It describes a collection of independent subsystems labelled by the wavevectors $\boldsymbol{k}$, and whose wavefunctions are $|\Psi_{\boldsymbol{k}}\rangle$. Each of these independent systems is in a superposition state involving the state $|\mathrm{vac}_{\boldsymbol{k}\uparrow,-\boldsymbol{k}\downarrow}\rangle$ (meaning that the Cooper pair $|\boldsymbol{k}\uparrow,-\boldsymbol{k}\downarrow\rangle$ is absent) with the probability amplitude u_k, and the state $|\boldsymbol{k}\uparrow,-\boldsymbol{k}\downarrow\rangle$ (the Cooper pair is present) with the probability amplitude v_k.

The factorisation described above is only possible with the BCS state $|\Psi_{\mathrm{BCS}}\rangle$. It does not hold for the state $|\Psi_N\rangle$ with a fixed total number of particles. This is why $|\Psi_{\mathrm{BCS}}\rangle$ is more amenable to calculations and interpretations than $|\Psi_N\rangle$.

The coefficients u_k and v_k may be determined exactly in the case of vanishing interactions ($a=0$). In this limit, the N–particle system consists of a Fermi sea defined by the Fermi wavevector $k_F=(3\pi^2 n)^{1/3}$, where n is the spatial density (cf. Problem 2, the different numerical prefactor reflects the fact that all single–particle states may now be populated by two particles with the internal states $|\uparrow\rangle$ and $|\downarrow\rangle$). Then, below the Fermi surface, all single–particle states are occupied, so that $u_k=0$ and $v_k=1$; above the Fermi surface, all single–particle states are empty, meaning that $u_k=1$ and $v_k=0$.

3.4 Statistics of the number of particles in the BCS state

In order to determine the statistics of the total atom number $\hat{N}$ in this state, we follow a procedure similar to the one we employed in Problem 1 when calculating the photon or electron number statistics in two–particle interference experiments. More precisely, we first calculate the properties of the atom number $\hat{n}_{\boldsymbol{k}}=\hat{n}_{\boldsymbol{k}\uparrow}+\hat{n}_{-\boldsymbol{k}\downarrow}$ for a given wavevector $\boldsymbol{k}$, and then use the independence of the random variables $n_{\boldsymbol{k}}$ to conclude as to the properties of $\hat{N}=\sum_{\boldsymbol{k}}\hat{n}_{\boldsymbol{k}}$.

The random variable $n_{\boldsymbol{k}}$ takes the value 0 with probability $|u_k|^2$, and the value 2 with the probability $|v_k|^2$ (the value is 2 and not 1 because each Cooper pair contains two particles). Therefore, its mean value is $\langle\hat{n}_{\boldsymbol{k}}\rangle=2|v_k|^2$. Similarly, the random variable $n_{\boldsymbol{k}}^2$ takes the value 0 with the probability $|u_k|^2$, and the value $2^2=4$ with the probability $|v_k|^2$, so that its mean value is $\langle\hat{n}_{\boldsymbol{k}}^2\rangle=4|v_k|^2$. Therefore, the variance of the random variable $n_{\boldsymbol{k}}$ is:

$$\Delta n_{\boldsymbol{k}}^2=\langle n_{\boldsymbol{k}}^2\rangle-\langle n_{\boldsymbol{k}}\rangle^2\quad=4(|v_k|^2-|v_k|^4)\quad=4|u_k|^2|v_k|^2\ , \tag{32}$$

where the last step follows from the normalisation condition $|u_k|^2+|v_k|^2=1$.

Now, we recall that $\hat{N}=\sum_{\boldsymbol{k}}\hat{n}_{\boldsymbol{k}}$. The random variables $n_{\boldsymbol{k}}$ are independent, so that the mean value $N=\langle\hat{N}\rangle$ of the particle number and its variance $\Delta N^2=\langle\hat{N}^2\rangle-\langle\hat{N}\rangle^2$ satisfy:

$$\langle\hat{N}\rangle=\sum_{\boldsymbol{k}}\langle n_{\boldsymbol{k}}\rangle=2\sum_{\boldsymbol{k}}|v_k|^2\quad\text{and}\quad\Delta N^2=\sum_{\boldsymbol{k}}\Delta n_{\boldsymbol{k}}^2=4\sum_{\boldsymbol{k}}|u_k|^2|v_k|^2\ . \tag{33}$$

Finally, we show that for large particle numbers N, the fluctuation ΔN of the particle number is small. For each wavevector $\boldsymbol{k}$, the normalisation $|u_k|^2+|v_k|^2=1$ entails that $|u_k|^2\le 1$. Combining this inequality with the expression for ΔN^2 in Eq. (33), we obtain:

$$\Delta N^2\le 4\sum_{\boldsymbol{k}}|v_{\boldsymbol{k}}|^2=2\,\langle\hat{N}\rangle\ ,\quad\text{so that}\quad\frac{\Delta N}{\langle\hat{N}\rangle}\le\sqrt{\frac{2}{\langle\hat{N}\rangle}}\ . \tag{34}$$

The second inequality in Eq. (34) shows that $\Delta N/N$ becomes arbitrarily small for sufficiently large N. Therefore, for large mean atom numbers, the fluctuations of the atom number in the BCS state are negligible, meaning that in the large–N limit the state $|\Psi_{\mathrm{BCS}}\rangle$ should capture the physics of a system containing a fixed number of particles (i.e. described by the wavefunction $|\Psi_N\rangle$).

4 Complement: The BCS ground state through a variational approach

Section 2.2 of the problem presents the analysis of the BCS Hamiltonian H_{BCS} in terms of the Bogoliubov approach [6, chap. 5]. This approach is applicable both to the homogeneous gas and to inhomogeneous systems, i.e. in the presence of a trapping potential $V(\boldsymbol{r})$. It involves three steps:

1. First, one exploits off–diagonal long–range order to replace the quartic Hamiltonian H_{BCS} by an approximate quadratic Hamiltonian.
2. Second, Bogoliubov rotations, parametrised by the coefficients u_k and v_k, are applied to the operators $c_{\boldsymbol{k}\uparrow}$ and $c^\dagger_{-\boldsymbol{k}\downarrow}$ to diagonalise this quadratic Hamiltonian.
3. Third, the coefficients u_k and v_k are interpreted as those appearing in Eq. (30), i.e. they define the Fourier coefficient ϕ_k of the pair wavefunction $\phi(\boldsymbol{r}_1,\boldsymbol{r}_2)$.

The case of a uniform Fermi gas ($V(\boldsymbol{r}) = 0$) allows for a more direct approach, which relies on a variational argument. In this approach, one chooses the coefficients u_k and v_k appearing in Eq. (30) so as to minimise the grand–canonical energy $\langle \Psi_{\rm BCS} | H_{\rm BCS} - \mu \hat{N} | \Psi_{\rm BCS} \rangle$. This yields the same values for u_k and v_k as the Bogoliubov approach presented in the problem.

In this variational approach, we start from the expression for $H_{\rm BCS}$ which appears as Eq. 10 in the problem. Substracting from it the operator $\mu \hat{N}$, we obtain the grand–canonical Hamiltonian:

$$H_{\rm BCS} - \mu \hat{N} = \sum_{\boldsymbol{k}} (\epsilon_k - \mu) \left(c^\dagger_{\boldsymbol{k}\uparrow} c_{\boldsymbol{k}\uparrow} + c^\dagger_{-\boldsymbol{k}\uparrow} c_{-\boldsymbol{k}\uparrow} \right) + \frac{g}{\Omega} \sum_{\boldsymbol{k},\boldsymbol{k'}} c^\dagger_{\boldsymbol{k}\uparrow} c^\dagger_{-\boldsymbol{k}\downarrow} c_{\boldsymbol{k'}\downarrow} c_{-\boldsymbol{k'}\uparrow} \ . \tag{35}$$

In the spirit of the Hilbert space decomposition of Eq. (21), we replace the sum over $\boldsymbol{k'}$ by a sum over $-\boldsymbol{k'}$. We also split the double sum over $\boldsymbol{k}$ and $\boldsymbol{k'}$ according to whether the two wavevectors are equal or different, and exploit the anticommutation rules in the case of equal wavevectors:

$$H_{\rm BCS} - \mu \hat{N} = \sum_{\boldsymbol{k}} (\epsilon_k - \mu) \left(c^\dagger_{\boldsymbol{k}\uparrow} c_{\boldsymbol{k}\uparrow} + c^\dagger_{-\boldsymbol{k}\uparrow} c_{-\boldsymbol{k}\uparrow} \right) + \frac{g}{\Omega} \sum_{\boldsymbol{k}} c^\dagger_{\boldsymbol{k}\uparrow} c_{\boldsymbol{k}\uparrow} c^\dagger_{-\boldsymbol{k}\downarrow} c_{-\boldsymbol{k}\downarrow} + \frac{g}{\Omega} \sum_{\boldsymbol{k} \neq \boldsymbol{k'}} c^\dagger_{\boldsymbol{k}\uparrow} c^\dagger_{-\boldsymbol{k}\downarrow} c_{-\boldsymbol{k'}\downarrow} c_{\boldsymbol{k'}\uparrow} \ . \tag{36}$$

The first two sums in Eq. (36) do not mix the subspaces $\mathcal{H}_{\boldsymbol{k}}$ of Eq. (21). In order to evaluate their average, we split the wavefunction $|\Psi_{\rm BCS}\rangle$ into two terms $|\Psi_{\boldsymbol{k}0}\rangle$ and $|\Psi_{\boldsymbol{k}1}\rangle$, corresponding to the cases where the pair $(\boldsymbol{k}\uparrow, -\boldsymbol{k}\downarrow)$ is absent or present, respectively. Thanks to Eq. (30):

$$|\Psi_{\rm BCS}\rangle = u_k \, |\Psi_{\boldsymbol{k}0}\rangle + v_k \, |\Psi_{\boldsymbol{k}1}\rangle \ . \tag{37}$$

Using this decomposition, one finds that the average of the kinetic energy term related to the wavevector $\boldsymbol{k}$ is $2(\epsilon_k - \mu) v_k^2$, and the average of the interaction term for $\boldsymbol{k} = \boldsymbol{k'}$ is $(g/\Omega) v_k^2$.

The third sum in Eq. (36) mixes two subspaces $\mathcal{H}_{\boldsymbol{k}}$ and $\mathcal{H}_{\boldsymbol{k'}}$ with $\boldsymbol{k} \neq \boldsymbol{k'}$. In order to evaluate its average, we split the wavefunction $|\Psi_{\rm BCS}\rangle$ into four terms $|\Psi_{\boldsymbol{k}0\boldsymbol{k'}0}\rangle$, $|\Psi_{\boldsymbol{k}0\boldsymbol{k'}1}\rangle$, $|\Psi_{\boldsymbol{k}1\boldsymbol{k'}0}\rangle$, $|\Psi_{\boldsymbol{k}1\boldsymbol{k'}1}\rangle$, describing the absence or the presence of the two pairs $(\boldsymbol{k}\uparrow, -\boldsymbol{k}\downarrow)$ and $(\boldsymbol{k'}\uparrow, -\boldsymbol{k'}\downarrow)$:

$$|\Psi_{\rm BCS}\rangle = u_k u_{k'} \, |\Psi_{\boldsymbol{k}0\boldsymbol{k'}0}\rangle + u_k v_{k'} \, |\Psi_{\boldsymbol{k}0\boldsymbol{k'}1}\rangle + v_k u_{k'} \, |\Psi_{\boldsymbol{k}1\boldsymbol{k'}0}\rangle + v_k v_{k'} \, |\Psi_{\boldsymbol{k}1\boldsymbol{k'}1}\rangle \ . \tag{38}$$

Using this decomposition, one finds that the average of the interaction term corresponding to $\boldsymbol{k} \neq \boldsymbol{k'}$ is $(g/\Omega) u_k v_k u_{k'} v_{k'}$. Combining the averages for all three sums in Eq. (36), we obtain:

$$\langle \Psi_{\rm BCS} | H_{\rm BCS} - \mu \hat{N} | \Psi_{\rm BCS} \rangle = \sum_{\boldsymbol{k}} \left(\epsilon_k - \mu + \frac{g}{\Omega} \right) v_k^2 + \frac{g}{\Omega} \sum_{\boldsymbol{k} \neq \boldsymbol{k'}} u_k u_{k'} v_k v_{k'} \ . \tag{39}$$

The interaction terms for $\boldsymbol{k} = \boldsymbol{k'}$ shift the chemical potential by $|g|/\Omega$. In the BCS limit, this shift is negligible compared to $\mu \sim E_F$, so that the average grand–canonical energy finally reduces to:

$$\langle \Psi_{\rm BCS} | H_{\rm BCS} - \mu \hat{N} | \Psi_{\rm BCS} \rangle = \sum_{\boldsymbol{k}} (\epsilon_k - \mu) \, v_k^2 \ + \ \frac{g}{\Omega} \sum_{\boldsymbol{k} \neq \boldsymbol{k'}} u_k u_{k'} v_k v_{k'} \ . \tag{40}$$

In order to minimise Eq. (40), we recall that $u_k^2 + v_k^2 = 1$. Hence, we let $u_k = \cos\theta_k$ and $v_k = \sin\theta_k$, and write Eq. (40) in terms of the angles θ_k:

$$\langle \Psi_{\rm BCS} | H_{\rm BCS} - \mu \hat{N} | \Psi_{\rm BCS} \rangle = \frac{1}{2} \sum_{\boldsymbol{k}} (\epsilon_k - \mu) \left[1 - \cos(2\theta_k) \right] \ + \ \frac{1}{4} \frac{g}{\Omega} \sum_{\boldsymbol{k} \neq \boldsymbol{k'}} \sin(2\theta_k) \sin(2\theta_{k'}) \ . \tag{41}$$

Derivating Eq. (41) with respect to θ_k, we obtain the minimisation conditions:

$$(\epsilon_k - \mu) \tan(2\theta_k) = -\frac{1}{2} \frac{g}{\Omega} \sum_{\boldsymbol{k'} \neq \boldsymbol{k}} \sin(2\theta_{k'}) \ . \tag{42}$$

We introduce the gap parameter Δ, defined as an average in the state $|\Psi_{\rm BCS}\rangle$:

$$\Delta = \frac{g}{\Omega} \sum_{\boldsymbol{k}} \langle \Psi_{\rm BCS} | c_{\boldsymbol{k}\uparrow} c_{-\boldsymbol{k}\downarrow} | \Psi_{\rm BCS} \rangle \quad = -\frac{g}{\Omega} \sum_{\boldsymbol{k}} u_k v_k \quad = -\frac{1}{2} \frac{g}{\Omega} \sum_{\boldsymbol{k}} \sin(2\theta_k) \ , \tag{43}$$

where the second equality follows from Eq. (37). Combining Eqs. (42) and (43):

$$\left(\epsilon_k - \mu - \frac{1}{2} \frac{g}{\Omega} \cos(2\theta_k) \right) \tan(2\theta_k) = \Delta \ . \tag{44}$$

We again neglect $|g|/\Omega$ compared to μ on the left–hand side, and obtain:

$$\tan(2\theta_k) = \frac{\Delta}{\epsilon_k - \mu} \ , \tag{45}$$

from which we extract the absolute values $\cos(2\theta_k)$ and $|\sin(2\theta_k)|$:

$$|\cos(2\theta_k)| = \frac{|\epsilon_k - \mu|}{E_k} \quad \text{and} \quad |\sin(2\theta_k)| = \frac{|\Delta|}{E_k} \ , \quad \text{where} \quad E_k = \sqrt{(\epsilon_k - \mu)^2 + \Delta^2}. \tag{46}$$

We choose the sign of $\cos(2\theta_k)$ to ensure the convergence of the average total number of particles:

$$N = \sum_{\boldsymbol{k}} \langle \Psi_{\rm BCS} | c^\dagger_{\boldsymbol{k}\uparrow} c_{\boldsymbol{k}\uparrow} + c^\dagger_{-\boldsymbol{k}\downarrow} c_{-\boldsymbol{k}\downarrow} | \Psi_{\rm BCS} \rangle \quad = \sum_{\boldsymbol{k}} 2 v_k^2 \ , \tag{47}$$

where the last step follows from the decomposition of Eq. (37). In order for the sum of Eq. (47) to converge, the coefficients v_k must go to zero for large $k = |\boldsymbol{k}|$. Therefore,

$$\text{For large } k, \quad \cos(2\theta_k) = \cos^2\theta_k - \sin^2\theta_k = u_k^2 - v_k^2 > 0 \ . \tag{48}$$

We expect $\Delta > 0$; additionally, for large k, $\epsilon_k - \mu > 0$. Hence, $\cos(2\theta_k)$ and $\sin(2\theta_k)$ satisfy:

$$\cos(2\theta_k) = +\frac{\epsilon_k - \mu}{E_k} \quad \text{and} \quad \sin(2\theta_k) = +\frac{\Delta}{E_k} \ . \tag{49}$$

Using $\cos^2\theta_k = [1 + \cos(2\theta_k)]/2$, $\sin^2\theta_k = [1 - \cos(2\theta_k)]/2$, and $\cos\theta_k \sin\theta_k = \sin(2\theta_k)/2$:

$$u_k^2 = 1 - v_k^2 = \frac{1}{2}\left(1 + \frac{\epsilon_k - \mu}{E_k}\right) \quad \text{and} \quad u_k v_k = \frac{\Delta}{2E_k} \ , \tag{50}$$

in accordance with Eq. 18 in the problem.

5 Chemical potential μ and gap Δ in terms of a and N

The BCS model is parametrised by two key quantities: the chemical potential μ and the gap Δ. Our last step is to relate μ and Δ to two parameters which may be tuned experimentally: the scattering length a and the particle number N. This is done by simultaneously solving the gap equation and the number equation, which appear together as Eq. 22 in the problem set.

In the BCS limit, the interaction between the particles is attractive and arbitrarily weak. This leads to a gap parameter Δ which is positive and very small. We shall make this assumption throughout this section and check its validity at the end of the calculation. In particular, we shall evaluate the integrals appearing in the gap and number equations to leading order in Δ/E_F.

5.1 Questions 22–23: Chemical potential μ

We start from the expression for the total number of particles given by Eq. (47) above. Replacing v_k^2 by its value given by Eq. (50), we obtain:

$$N = \sum_{\boldsymbol{k}} \left(1 - \frac{\epsilon_k - \mu}{E_k}\right) \quad = \int \frac{d^3k}{(2\pi)^3/\Omega} \left(1 - \frac{\epsilon_k - \mu}{E_k}\right) \ . \tag{51}$$

The gas is homogeneous, therefore its spatial density is $n = N/\Omega$:

$$n = \int \frac{d^3k}{(2\pi)^3} \left(1 - \frac{\epsilon_k - \mu}{E_k}\right) \ . \tag{52}$$

In Eq. (52), the integrand $f(\epsilon_k)$ is a function of $\epsilon_k = \hbar^2 k^2/(2m)$ only. Introducing the Fermi energy E_F and wavevector k_F, related through $E_F = \hbar^2 k_F^2/(2m)$, we change variables from d^3k to $d\epsilon$ in the integral using the general formula:

$$\int \frac{d^3k}{(2\pi)^3} f(\epsilon_k) = \frac{k_F^3}{4\pi^2} \int \frac{d\epsilon}{E_F} \left(\frac{\epsilon}{E_F}\right)^{1/2} f(\epsilon) \ . \tag{53}$$

Applying Eq. (53) to Eq. (52), we find:

$$n = \frac{k_F^3}{4\pi^2} \int \frac{d\epsilon}{E_F} \left(\frac{\epsilon}{E_F}\right)^{1/2} \left(1 - \frac{\epsilon_k - \mu}{E_k}\right) \ . \tag{54}$$

Replacing k_F by its expression for a Fermi gas with two accessible internal states, $k_F = (3\pi^2 n)^{1/3}$, the spatial density cancels out and we obtain:

$$\frac{4}{3} = \int_0^\infty \frac{d\epsilon}{E_F} \left(\frac{\epsilon}{E_F}\right)^{1/2} \left(1 - \frac{\epsilon - \mu}{E_k}\right) . \tag{55}$$

We consider the integral appearing in Eq. (55) in the limit where $\Delta \to 0$. In this limit, the excitation energy $E_k = \left[(\epsilon_k - \mu)^2 + \Delta^2\right]^{1/2}$ reduces to $E_k = |\epsilon_k - \mu|$. The content of the second pair of parentheses in Eq. (55) is equal to 2 for $\epsilon < \mu$, and equal to 0 for $\epsilon > \mu$. Therefore, Eq. (55) reduces to:

$$\frac{4}{3} = \int_0^\mu \frac{d\epsilon}{E_F} \left(\frac{\epsilon}{E_F}\right)^{1/2} 2 \quad = \frac{4}{3} \left(\frac{\mu}{E_F}\right)^{3/2} . \tag{56}$$

We conclude from Eq. (56) that $\mu = E_F$: In the BCS limit, the attractive interaction is so weak that it does not affect the chemical potential, which retains its non–interacting value.

5.2 Gap parameter Δ

5.2.1 Question 21: Integral equation for the gap Δ

We now turn to the gap parameter Δ, which we express in terms of the coefficients u_k and v_k thanks to Eq. (43) above. We replace $u_k v_k$ by its value given by Eq. (50):

$$\Delta = -\frac{g}{\Omega} \sum_{\boldsymbol{k}} u_k v_k = -\frac{g}{\Omega} \sum_{\boldsymbol{k}} \frac{\Delta}{2E_k} . \tag{57}$$

The gap Δ cancels out from Eq. (57) (although it is still present implicitly through E_k):

$$1 = -\frac{1}{2} \frac{g}{\Omega} \sum_{\boldsymbol{k}} \frac{1}{E_k} . \tag{58}$$

We replace the discrete sum appearing in Eq. (58) with an integral over the integration element is $d^3k \times \Omega/(2\pi)^3$:

$$-\frac{1}{g} \quad = \quad \int \frac{d^3k}{(2\pi)^3} \frac{1}{2E_k} . \tag{59}$$

In Eq. (59), we express the coupling constant g in terms of the scattering length a through $g = 4\pi\hbar^2 a/m$, and use the relation $E_k = [(\epsilon_k - \mu)^2 + \Delta^2]^{1/2}$ (see Eq. 18 in the problem set) to obtain:

$$-\frac{\pi}{2\, k_F a} \quad = \quad \int \frac{dk\, k^2}{k_F^3} \frac{E_F}{[(\epsilon_k - \mu)^2 + \Delta^2]^{1/2}} . \tag{60}$$

The integral appearing on the right–hand side of Eq. (60) *does not converge* for large momenta, in which limit the integrand tends to a constant. This reflects the pathological behaviour of the contact potential $g\delta(\boldsymbol{r})$, whose Fourier transform does not fall off for large momenta. An accurate determination of the gap parameter Δ requires a more elaborate analysis of the relation between g and a, sketcked e.g. in Ref. [7, Sec. 26.5.2] (see in particular their Eqs. 26.33 and 26.34). We shall not address this issue, and rely instead on a standard, but approximate, approach involving a truncation of the integral. Therefore, our final expression for the gap Δ should not be expected to be entirely correct (see Eq. (65) below and the discussion of its shortcomings).

5.2.2 Question 24: Approximate evaluation of the integral giving the gap Δ

Using Eq. (53) above, we change variables in Eq. (60) to integrate over the single–particle energy ϵ. This leads to:

$$-\frac{\pi}{2\, k_F a} \quad = \quad \frac{1}{2} \int \frac{d\epsilon}{E_F} F_\Delta(\epsilon) , \quad \text{with} \quad F_\Delta(\epsilon) = \left[\frac{\epsilon/E_F}{[(\epsilon/E_F - 1)^2 + (\Delta/E_F)^2]}\right]^{1/2} . \tag{61}$$

The integrand F_Δ in Eq. (61) depends on two adimensional quantities: ϵ/E_F and the parameter Δ/E_F. It is represented on Fig. 2. It is strongly peaked near $\epsilon = E_F$, the peak being more pronounced for smaller values of Δ/E_F.

In Eq. (61), The strongly peaked structure of $F_\Delta(\epsilon)$ allows us to replace ϵ by E_F in the numerator of the square root in the integral on the right–hand side of Eq. (61). We change the integration variable from ϵ to $\eta = \epsilon - E_F$.

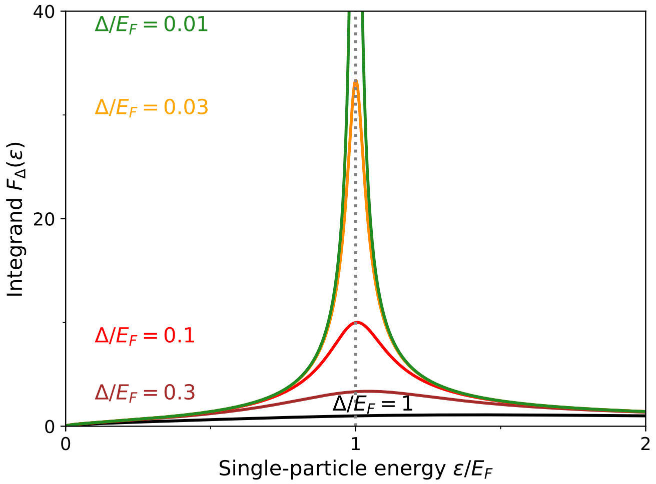

Figure 2 The integrand $F_\Delta(\epsilon)$ of Eq. (61), represented as a function of the single–particle energy ϵ/E_F, for various values of the adimensional ratio Δ/E_F. It is strongly peaked in the vicinity of the Fermi momentum $k = k_F$. The peak is more pronounced for smaller values of Δ/E_F.

Furthermore, as anticipated at the end of the previous section 5.2.1, we introduce an energy cut–off $\bar{\epsilon}$. The value of $\bar{\epsilon}$ is chosen of the order of the Debye frequency $\hbar\omega_D$. This reflects the fact that the interaction by phonon exchange in the weakly–interacting Fermi gas involves only particles in a comparatively thin shell of $\boldsymbol{p}$–space near the Fermi surface, whose thickness $\hbar\omega_D$ is small in comparison with the chemical potential $\mu = E_F$. Hence, Eq. (61) reduces to:

$$-\frac{\pi}{2\,k_F a} = \frac{1}{2}\int_{-\bar{\epsilon}}^{+\bar{\epsilon}} \frac{d\eta}{E_F}\,\frac{E_F}{[\eta^2+\Delta^2]^{1/2}} = \int_{0}^{+\bar{\epsilon}} \frac{d\eta}{E_F}\,\frac{E_F}{[\eta^2+\Delta^2]^{1/2}}\ , \tag{62}$$

where the last step follows from the integrand being an even function of η. Changing variables to $u = \eta/\Delta$ yields:

$$-\frac{\pi}{2\,k_F a} = \int_{0}^{+\bar{\epsilon}/\Delta} \frac{du}{(1+u^2)^{1/2}} = \operatorname{arcsinh}(\bar{\epsilon}/\Delta)\ . \tag{63}$$

Recalling that $a < 0$, so that $-a = |a|$, we rewrite Eq. (63) as:

$$\frac{\bar{\epsilon}}{\Delta} = \sinh\left(\frac{\pi}{2k_F|a|}\right) = \frac{1}{2}\left[\exp\left(+\frac{\pi}{2k_F|a|}\right) + \exp\left(-\frac{\pi}{2k_F|a|}\right)\right]\ , \tag{64}$$

where the last step exploits the definition of the function sinh. Recalling the assumption that $k_F|a|$ is small, the second exponential term (negative argument) is negligible compared to the first one (positive argument). We finally obtain:

$$\frac{\bar{\epsilon}}{\Delta} = \frac{1}{2}\exp\left(+\frac{\pi}{2k_F|a|}\right)\ ,\qquad \text{or, equivalently,}\qquad \Delta = 2\bar{\epsilon}\,\exp\left(-\frac{\pi}{2k_F|a|}\right)\ . \tag{65}$$

Equation (65) is the famous result of BCS theory which expresses the gap parameter Δ in terms of the scattering length a, and more precisely in terms of the adimensional parameter $k_F a$. This equation validates the two assumptions we had made on Δ throughout the calculation: First, $\Delta > 0$. Second, in the deep BCS regime where $k_F a$ is negative and small, the exponential is extremely small, so that $\Delta \ll E_F$. One may also verify that the many–body state defined by Eq. (30) is indeed energetically favoured compared to the non–interacting ground state [1, §4.6.1]

The approximate approach involving the cut–off energy $\bar{\epsilon}$ provides the correct exponent in Eq. (65), but not the correct prefactor. In fact, the approximate nature of Eq. (65) is easily seen from the fact that the prefactor it involves, $2\bar{\epsilon}$, depends on the cut–off energy $\bar{\epsilon}$. The more elaborate approach mentioned at the end of Sec. 5.2.1 yields the exact result $\Delta/E_F = (8/e^2)\exp\left[-\pi/(2k_F|a|)\right]$, which involves no dependence on any cut–off parameter.

6 Question 25: Validity and experimental considerations

6.1 The BEC–BCS crossover

This problem has explored the BCS model applied in the BCS limit, i.e. $k_F a$ negative and small. However, the model it presents is also applicable in the deep BEC regime, i.e. $k_F a$ positive and small. The BCS model is a mean–field theory[6], therefore it cannot be expected to provide an accurate solution in the strongly–correlated regime where

---

[6] In the Bogoliubov treatment outlined in the problem, the mean–field approximation intervenes when one replaces the BCS Hamiltonian of Eq. (35), which is of order 4 in the operators $c_{\boldsymbol{k}\sigma}$ and $c^\dagger_{\boldsymbol{k}\sigma}$, by the quadratic Hamiltonian H_{eff} (cf. question 12).

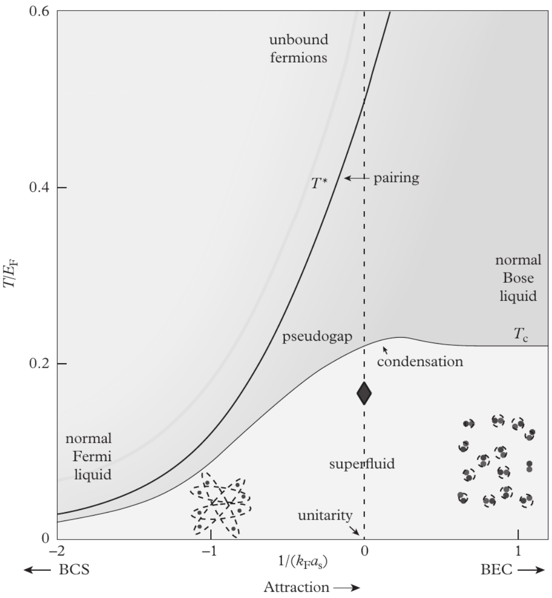

Figure 3 Critical temperature for superfluidity along the BEC–BCS crossover. The smooth solid line labelled "condensation" results from the BCS approach discussed in the problem. The diamond indicates the value of T_c/T_F in the unitary regime obtained using numerical quantum Monte Carlo calculations. Reproduced from Ref. [8].

$k_F|a| \gtrsim 1$. Nevertheless, it provides useful orders of magnitude, and in the context of this model all thermodynamic functions vary smoothly when $1/(k_F a)$ is varied along the crossover from the BCS to the BEC regimes [8, §16.7].

Among these thermodynamic quantites, the critical temperature T_c below which the system is superfluid is an important example. The order of magnitude for T_c is dictated by the gap: $k_B T_c \sim \Delta$, with k_B being Boltzmann's constant. An improved approximation may be obtained by solving the BCS equations at non–zero temperature [1, §4.8]. The resulting adimensional ratio T_c/T_F is represented as a function of $1/(k_F a)$ on Fig. 3 (solid line labelled 'condensation').

The two weakly–interacting limits for the critical temperature T_c are well–understood. First, for $k_F a$ small and negative, the BCS theory yields:

$$k_B T_c^{\mathrm{BCS}} = \frac{e^\gamma}{\pi}\,\Delta(T=0)\ , \tag{66}$$

where $\gamma \approx 0.577$ is Euler's constant, and $\Delta(T=0)$ is the zero–temperature value of the gap, which is given by Eq. (65) and is exponentially small. Second, for $k_F a$ small and positive, the pairs are tightly–bound bosonic molecules, and the critical temperature is given by the standard formula for a uniform Bose gas, with the mass of a single boson being $m_{\mathrm{mol}} = 2m$ and the bosonic density being $n_{\mathrm{mol}} = n/2$:

$$n_{\mathrm{mol}}\,\Lambda_{T_c}^3 = \zeta(3/2)\ . \tag{67}$$

In Eq. (67), $\Lambda_T = [2\pi\hbar^2/(m_{\mathrm{mol}} k_B T)]^{1/2}$ is the thermal de Broglie wavelength and $\zeta(3/2) = \sum 1/n^{3/2} \approx 2.61$. Solving Eq. (67) for T_c, one obtains the critical temperature in the BEC limit:

$$\frac{k_B T_c^{\mathrm{BEC}}}{E_F} = \left(\frac{2}{\pi}\,\frac{1}{[3\zeta(3/2)]^2}\right)^{1/3} \quad \approx 0.218\ . \tag{68}$$

The investigation of the strongly–interacting regime is much more challenging. The prediction of the BCS model is smooth but non–monotonic near the unitary limit where $1/(k_F a) = 0$ (see the solid curve on Fig. 3). In the regime where $|k_F a| \gtrsim 1$, mean–field theories are expected to be inaccurate, and at present no exact solution for the many–body problem is available. Therefore, one turns to more involved numerical Quantum Monte Carlo calculations, which yield the following universal[7] result for $1/(k_F a) = 0$ (see e.g. Ref. [8, §16.6]):

$$\frac{k_B T_c^{\mathrm{unitarity}}}{E_F} \approx 0.167\ , \tag{69}$$

which is in excellent agreement with recent experimental results [9], but is slightly below the mean–field prediction, thus confirming that the latter is not sufficiently accurate.

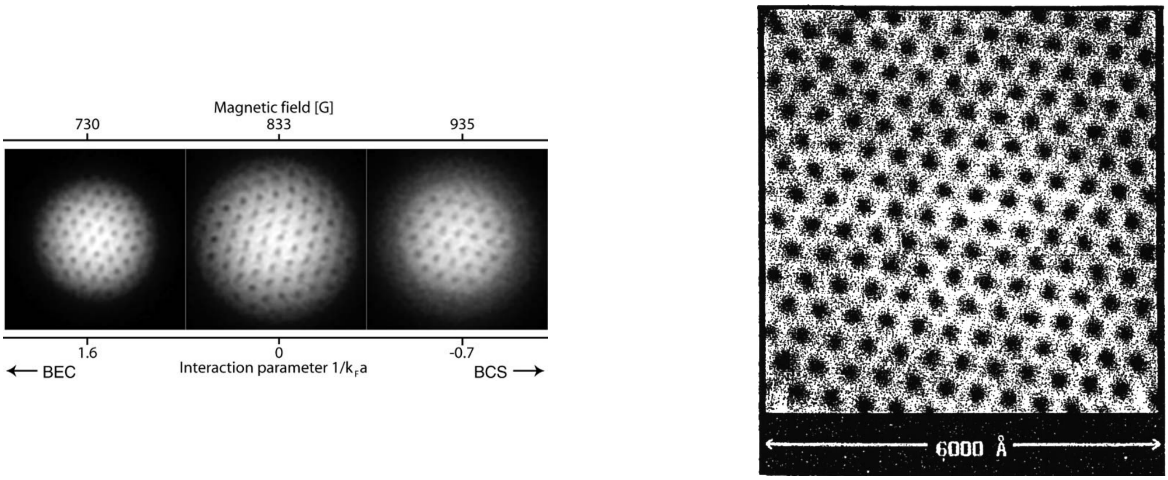

Figure 4 **Left:** Abrikosov lattice of vortices observed by scanning tunnelling microscopy in the superconductor $\mathrm{NbSe_2}$, which exhibits BCS superconductivity for $T < T_c = 7.2\,\mathrm{K}$. Reproduced from Ref. [10]. **Right:** Experimental proof of superfluidity in an interacting ultracold gas of fermionic ^{6}Li: Abrikosov lattices of vortices have been nucleated and observed for $1/(k_F a) = 1.6$ (BEC regime), $1/(k_F a) = 0$ (unitary regime), and $1/(k_F a) = -0.7$ (BCS regime). Reproduced from Ref. [1].

6.2 Observation of Abrikosov lattices

The observation of vortex lattices in interacting Fermi gases (see e.g. Ref. [1, Sec. 6.6]) has provided spectacular experimental proof of their superfluid character. As illustrated on the right panel of Fig. 4, these lattices have been nucleated for various values of a in the BEC regime ($1/(k_F a) = 1.6$), at unitarity ($1/(k_F a) = 0$), and in the BCS regime ($1/(k_F a) = -0.7$). For these values of the interaction parameter $1/(k_F a)$, Eqs. (68) and (69) show that the critical temperature is of the order of a few tenths of the Fermi energy, so that $T_c \sim 200\,\mathrm{nK}$, a temperature which is nowadays routinely accessed experimentally. However, bringing a Fermi gas deep into the BCS regime is an experimental challenge because of the exponentially small critical temperature in the BCS limit (see Eq. (66)). To the best of my knowledge, this challenge remains to be met. For now, the equivalent of the very deep BCS regime on the far left of Fig. 3 is more easily accessed in condensed–matter systems, i.e. metallic superconductors, where T_c^{BCS} is of the order of a few Kelvin. For example, the left panel of Fig. 4 shows a vortex lattice observed by scanning tunnelling microscopy in niobium diselenide, whose critical temperature is $T_c = 7.2\,\mathrm{K}$, in the presence of a magnetic field.

References

[1] W. Ketterle, M. Zwierlein, in *Proceedings of the International School of Physics Enrico Fermi, course CLXIV (Varenna, June 2006)* (2008).

[2] N. W. Ashcroft, N. D. Mermin, *Solid State Physics*, Harcourt (1976).

[3] K. M. Jones, E. Tiesinga, P. D. Lett, P. Julienne, Rev. Mod. Phys. **78**, 483 (2006).

[4] C. Cohen-Tannoudji, B. Diu, F. Laloë, *Quantum Mechanics, volume II*, Wiley, 2nd ed. (2020).

[5] C. Chin, R. Grimm, P. Julienne, E. Tiesinga, Rev. Mod. Phys. **82**, 1225 (2010).

[6] P. G. de Gennes, *Superconductivity of metals and alloys*, Addison-Wesley (1966).

[7] C. Cohen-Tannoudji, D. Guéry-Odelin, *Advances in atomic physics: an overview*, World Scientific (2011).

[8] L. P. Pitaevskii, S. Stringari, *Bose-Einstein condensation and superfluidity*, Oxford University Press, 2nd ed. (2016).

[9] M. J. H. Ku, A. T. Sommer, L. W. Cheuk, M. W. Zwierlein, Science **335**, 563 (2012).

[10] A. A. Abrikosov, Rev. Mod. Phys. **76**, 975 (2004).

---

[7] The unitary Fermi gas is defined by two conditions: *(i)* $k_F\, r_0 \ll 1$, where r_0 is the range of the interaction potential, meaning that the system is dilute; and *(ii)* $|k_F\, a| \gg 1$, meaning that the system is strongly–interacting. In this limit, the scattering length a is no longer a relevant lengthscale: the only remaining dimensional parameter is the Fermi energy E_F. Therefore, the adimensional ratio $k_B T_c^{\mathrm{unitarity}}/E_F$ is a universal number.